(iii) In general, whenever a mode is cut off, its effect is also easily included by terminating the appropriate port in Fig. 3 with a reactive impedance.

(iv) As a particular case, the transitions presented in [1 – 5] with an open-ended slot (Fig. 1*b*) and an air-bridge at the transition plane can be analysed by connecting a short-circuit (air-bridge) to port 3 in Fig. 3, and letting $Z_A \rightarrow \infty$.

(v) Since the model contains circuit elements, it enables the energy transfer from one mode to any other mode in the transition to be quantitatively analysed, and can be easily implemented in microwave CAD.

Model application and experimental validation: The proposed model has been applied to a K-band (18–26.5GHz) slotline resonator fabricated on CuClad 217, $\varepsilon_r = 2.17$, thickness = 0.254mm. (see Fig. 4*a*) and placed in the *E*-plane of a WR-42 rectangular waveguide. The resonator consists of a CPW section loaded with two slotline-to-CPW asymmetrical transitions ($Z_A \simeq 0$ in Fig. 2). The slotline width and resonator slotwidth are 0.2mm. The resonator length is 4.7mm. The separation between the slotline and resonator slot is 0.1mm. Figs. 4*a* and *b* show a composition of its simulated *S*-parameters (obtained using the model shown in Fig. 3 for each transition) with its measured *S*-parameters. The excellent agreement between simulations and measurements (the model accurately predicts the resonance frequency) demonstrates the validity of the model and applicability.

Conclusions: A new 'circuit model' for slotline-to-coplanar waveguide asymmetrical transitions that separates the contributions of CPW modes into different ports has been proposed. The model overcomes limitations of previous models, because it enables a general case to be analysed in which air-bridges are not present, and slot-terminating impedances other than an open circuit can be used. It has been successfully applied to the analysis of slotline resonators, showing excellent agreement with experimental results.

Acknowledgment: This work has been supported by the research project TIC97-1129-C04-04 financed by the Spanish Government CICYT.

21 May 1999

Electronics Letters Online No: 19990779

DOI: 10.1049/el:19990779

M. Ribó (*Enginyeria La Salle - Ramon Llull University (URL), Dept. CTS, Pg. Bonanova 8, 08022 Barcelona, Spain*)

J. de la Cruz and L. Pradell (*Polytechnic University of Catalunya (UPC), Dept. TSC, Campus Nord UPC, 08034 Barcelona, Spain*)

References

1 WANG, T., OU, Z., and WU, K.: 'Experimental study of wideband uniplanar phase inverters for MIC'. MTT-S Int. Microwave Symp. Dig., 1997, pp. 777–780

2 YANEV, A.S., TODOROV, B.N., and RANEV, V.Z.: 'A broad-band balanced HEMT frequency doubler in uniplanar technology', *IEEE Trans.*, 1998, **MTT-46**, (12), pp. 2032–2034

3 CHIOU, H.-K., CHANG, C.-Y., and LIN, H.-H.: 'Balun design for uniplanar broadband double balanced mixer', *Electron. Lett.*, 1995, **31**, (24), pp. 2113–2114

4 HSU, P.-C., NGUYEN, C. , and KINTIS, M.: 'A new uniplanar broadband singly balanced diode mixer', *IEEE Trans.*, 1998, **MTT-46**, (11), pp. 1782–1784

5 HSU, P.-C., NGUYEN, C., and KINTIS, M.: 'Uniplanar broad-band push-pull FET amplifiers', *IEEE Trans.*, 1997, **MTT-45**, (12), pp. 2150–2152

6 OMAR, A.S., and SCHÜNEMANN, K.: 'Realisations and design of fine-line bandstop filters'. Proc. 13th European Microwave Conf., 1983, pp. 157–162

Cascaded $\chi^{(2)}$ wavelength converter in $LiNbO_3$ waveguides with counter-propagating beams

I. Brener, M.H. Chou, D. Peale and M.M. Fejer

A wideband wavelength converter is presented which is based on a cascaded second-order nonlinearity in periodically-poled $LiNbO_3$ waveguides pumped at 1.5μm. The converter uses counter-propagating beams in order to improve conversion efficiency and pump rejection. An internal conversion efficiency of –10dB and a conversion bandwidth of 68nm have been obtained in a 4cm long device.

Introduction: Wavelength conversion at 1550nm is carried out in a variety of ways [1]. One attractive way of implementing wavelength conversion is by using difference frequency generation (DFG) in a nonlinear optical medium [2 – 4]. This process is instantaneous and optically transparent, has a negligible noise floor, and has no intrinsic frequency chirp. Multiple channels can also be converted simultaneously with equal efficiencies. However, DFG-based wavelength converters require a singlemode 50–150mW pump operating at roughly half the signal wavelength, i.e. ~780nm [2 – 4]. This also implies mode-matching complications in the nonlinear waveguide due to the use of very different wavelengths. A solution to this problem by the use of a cascaded $\chi^{(2)}$ process ($\chi^{(2)}$:$\chi^{(2)}$) has been proposed [5] and demonstrated [6] in periodically poled $LiNbO_3$ (PPLN) waveguides. We recently demonstrated a device based on a cascaded interaction with internal conversion efficiency of –8dB, pumped by a laser also in the 1550nm region [7]. The implementation of this device used co-propagating pump and signal beams. Thus, considerable pump power is present at the output of the waveguide and consequently an appropriate blocking filter must be used. In this Letter, we report a wavelength converter that uses counter-propagating pump and signal beams. This configuration improves the overall conversion efficiency and alleviates the pump rejection requirements.

The ($\chi^{(2)}$:$\chi^{(2)}$) device using counter-propagation beams is implemented by launching the pump and signal beams from opposite facets of the waveguide and coating one facet with a dichroic dielectric mirror that reflects the second harmonic beam back into the waveguide. In this device, the pump at frequency ω_p is up-converted to frequency $2\omega_p$ by second harmonic generation (SHG). The generated $2\omega_p$ is reflected back into the waveguide and mixes with the input signal ω_s for co-propagating phase-matching to generate a wavelength shifted output $\omega_{out} = 2\omega_p - \omega_s$ by DFG. Phase-matching between interacting waves for both SHG and DFG is required, and can be accomplished by choosing an appropriate quasi-phasematching (QPM) grating period. Phasematching with counter-propagating beams is in principle possible but the poling period required is extremely small (< 1μm) and cannot therefore be easily achieved in a practical device.

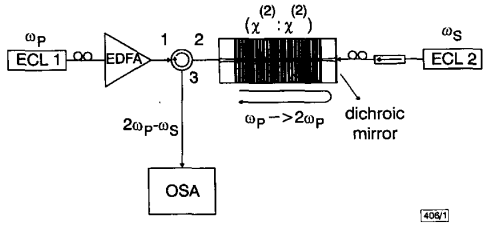

Fig. 1 *Experimental setup for counter-propagating beam wavelength converter based on cascaded $\chi^{(2)}$ nonlinearity*

ECL: external cavity laser; PPLN WG: periodically poled $LiNbO_3$ waveguide; EDFA: erbium-doped fibre amplifier; OSA: optical spectrum analyser

Fabrication: We fabricated the waveguides by annealed proton exchange in PPLN. The device used in this experiment is 4cm long, has a QPM period of 14.8μm, waveguide width of 12μm, proton exchange depth of 0.7μm, and was annealed for 26h at 325°C. We can tune the pump wavelength by using waveguides with different QPM period and/or temperature tuning. The

normalised efficiency of this device is 50–60%/Wcm^2. Efficient fibre coupling is achieved by introducing extra 1mm taper regions at the input and output of the waveguides. We then coated one facet by e-beam deposition with a dielectric six-layer stack of Al_2O_3 and Si. This mirror had a reflectivity of ~96% at 780nm and ~1% at 1550nm.

Experiment: Fig. 1 shows the experimental setup used in this work. The pump laser is an external cavity laser (ECL) amplified by an erbium-doped fibre amplifier (EDFA). The signal channel is provided by another ECL and is fibre launched from the coated side of the waveguide. The converted output is collected through a circulator. The total loss in the signal path, including isolator, coupling and propagation losses and circulator is 5.6dB; the waveguide-related losses are only ~3.3dB.

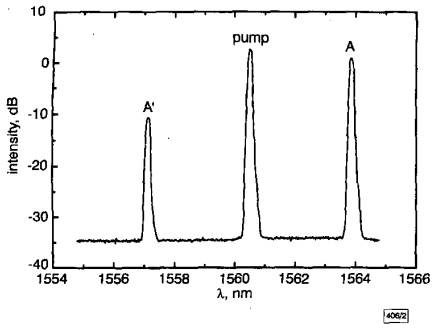

Fig. 2 *Typical trace measured at port 3 of circulator for single channel wavelength conversion*

Pump power ~120mW; note good rejection of remaining pump power due to counter-propagating geometry

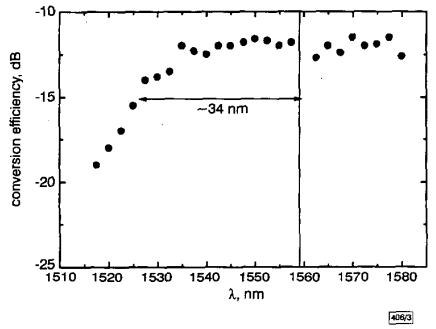

Fig. 3 *Bandwidth of wavelength conversion device measured for fixed pump wavelength*

Centre of bandwidth curve is given by wavelength of pump laser

A typical trace measured at port 3 of the circulator is shown in Fig. 2. The converted signal is denoted by A'. The pump power was 120mW and the input signal power was 6.5dBm. The main advantages of this device are clearly seen in this Figure: (i) the relatively high conversion efficiency (–12dB) with modest pump powers, (ii) a good suppression of the pump laser left after the conversion process, and (iii) low total losses in the signal path. Wavelength conversion with –10dB internal efficiency was achieved when the pump power was increased to 200mW. We then varied the signal wavelength and measured the conversion efficiency for a fixed pump wavelength (1559nm) and power (110mW). Fig. 3 shows the measured bandwidth of this wavelength converter. This device has a 3dB signal bandwidth of 68nm.

Fig. 4 presents a comparison of the fibre-to-fibre efficiency of a ($\chi^{(2)}$:$\chi^{(2)}$) wavelength converter using counter-propagation beams and a collinear device [7]. For this modelling we kept all the parameters the same, as follows: waveguide losses of 0.4 (0.7)dBcm at 1550 (780)nm; taper and coupling losses of 1.0dB; dichroic reflectivity of 98%, and pump power of +20 and +23dBm. These are all realistic parameters and we intentionally limit the pump power to such values as higher levels require a costly EDFA and the performance of the waveguides is degraded. We plot these efficiencies as a function of device length (devices longer than 8cm are not feasible; moreover, the pump bandwidth also becomes too narrow) and for several normalised conversion efficiencies. The counter-propagating device has a higher conversion efficiency than the collinear device, for lengths less than ~6cm: for shorter devices it is more advantageous to generate the SHG field first and then use it for DFG, as opposed to a simultaneous process as in the collinear device. Longer devices are dominated by waveguide losses and the situation is reversed. Finally, it should not be forgotten that the collinear geometry would in general have more losses at the input than the device shown in this Letter, since pump and signals have to be coupled through a fibre coupler. Finally, the device was linear (resolution 0.1dB) up to signal powers of 5dBm.

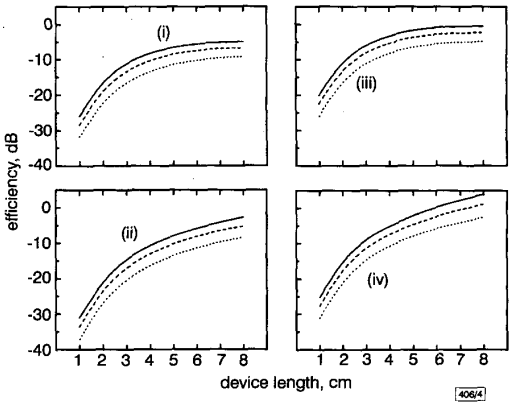

Fig. 4 *Fibre-to-fibre efficiency comparison of converted signal against device length for pump powers of 100 and 200mW*

Dichroic mirror reflectivity = 98%
(i) I_p = 100mW, counter-propagating device (A)
(ii) I_p = 200mW, co-propagating device (B)
(iii) I_p = 100mW, counter-propagating device (A)
(iv) I_p = 200mW, co-propagating device (B)
····· 50%/Wcm^2
– – – – 75%/Wcm^2
——— 100%/Wcm^2

In summary, we have presented a wavelength conversion device for 1550nm signals channels with a –10dB internal conversion efficiency, 68nm of conversion bandwidth and good linearity. This device uses a cascaded $\chi^{(2)}$ process in PPLN waveguides with counter-propagating pump and signal paths. This allows for improved conversion efficiency and reduces the need for strong pump blocking after the conversion process.

Acknowledgments: This work was sponsored by Lucent Technologies, JESP, and DARPA through the OMC; we also thank Crystal Technology.

6 April 1999
Electronics Letters Online No: 19990625
DOI: 10.1049/el:19990625

I. Brener and D. Peale (*Bell Laboratories, Lucent Technologies, 700 Mountain Avenue, Murray Hill, NJ 07974, USA*)

M.H. Chou and M.M. Fejer (*E.L. Ginzton Laboratory, Stanford University, Stanford, CA 94305-4085, USA*)

References

1 YOO, S.J.B.: 'Wavelength conversion technologies for WDM network applications', *J. Lightwave Technol.*, 1996, **LT-14**, pp. 955–966

2 YOO, S.J.B., KOZA, M.A., CANEAU, C., and BHAT, R.: 'Simultaneous wavelength conversion of 2.5-Gbit/s and 10-Gbit/s signal channels by difference-frequency generation in an AlGaAs waveguide'. Conf. Optical Fiber Communications, 1998, Vol. OSA Tech. Dig. Ser. 2, Paper WB5, pp. 106–107

3 XU, C.Q., OKAYAMA, H., and KAWAHARA, M.: '1.5 μm band efficient broadband wavelength conversion by difference frequency generation in a periodically domain-inverted $LiNbO_3$ channel waveguide', *Appl. Phys. Lett.*, 1993, **63**, pp. 3559–3561

4 CHOU, M.H., HAUDEN, J., ARBORE, M.A., and FEJER, M.M.: '1.5-μm-band wavelength conversion based on difference-frequency generation in $LiNbO_3$ waveguides with integrated coupling structures', *Opt. Lett.*, 1998, **23**, pp. 1004–1006

5 GALLO, K., ASSANTO, G., and STEGEMAN, G.: 'Efficient wavelength shifting over the erbium amplifier bandwidth via cascaded second order processes in lithium niobate waveguides', *Appl. Phys. Lett.*, 1997, **71**, pp. 1020–1022

6 TREVINO-PALACIOS, C.G., STEGEMAN, G.I., DE BALDI, P., and MICHELI, M.P.: 'Wavelength shifting using cascaded second-order processes for WDM applications at 1.55μm', *Electron. Lett.*, 1998, **34**, pp. 2157–2158

7 BRENER, I., CHOU, M.H., and FEJER, M.M.: 'Efficient wideband wavelength conversion using cascaded second-order nonlinearities in $LiNbO_3$ waveguides'. Conf. Optical Fiber Communications, 1999, Paper FB6

Operation of surface-tension self-assembled 3D micro-optomechanical torsion mirror scanner

R.R.A. Syms

The operation of an electrostatically-driven 3D micro-optomechanical resonant torsion mirror scanner is described. The device is fabricated in bonded silicon-on-insulator and self-assembled by out-of plane rotation powered by a surface tension torque obtained by melting photoresist. A scan angle of 16° is obtained at a drive frequency of 2.6kHz using a voltage of 175V.

Great interest has recently been shown in 3D silicon micro-opto-electro-mechanical systems (MOEMS), which have been demonstrated by several US groups (e.g. Berkeley Sensors and Actuators Center). They consist of polysilicon parts, fabricated using multilayer surface micromachining. The parts are attached to the substrate by hinges, rotated out-of-plane, and locked in position by a latch mechanism [1]. The parts can carry components such as lenses [2], and can be driven electrostatically or thermally to perform beam scanning operations [3, 4].

To date, these components have been assembled manually or by surface micromachined assembly engines such as linear vibromotors [5]. We have developed an alternative process, based on out-of-plane rotation powered by the surface tension of small pads of meltable material [6]. The mechanism is compact, and allows precise self-assembly operations to be carried out by heating. Here, we describe an electrostatically-driven 3D micro-optomechanical resonant torsion mirror scanner constructed in this way.

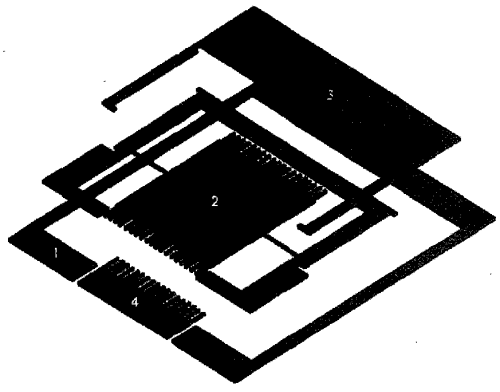

Fig. 1 *Layout of parts comprising torsion mirror scanner*

(1) base
(2) frame carrying mirror on torsion bar
(3) frame carrying latches
(4) fixed half of electrostatic comb drive

Fig. 1 shows an exploded view of the device, which contains four main components: a base (1), a frame carrying a mirror on a torsion bar (2), a frame carrying latches (3), and the fixed half of an electrostatic comb drive (4). The moving half of the comb drive is attached to the mirror. The parts are fabricated by surface micromachining of Si, and are initially parallel to the substrate. However, parts 1 and 4 are attached to the substrate by an insulating layer, while parts 2 and 3 are freed by etching this layer away. Self-assembly is carried out by rotating parts 2 and 3 simultaneously out-of-plane, using the torque obtained by melting small pads linking them to part 1. The latches ensure that assembly stops after 45° rotation of parts 2 and 3.

The device was constructed using a simple two-mask surface micromachining process based on bonded silicon-on-insulator (BSOI), and self-assembly was powered by photoresist. The BSOI was obtained from BCO (NI) Ltd. and consisted of 4" (100) Si substrates carrying a 6 μm thick bonded Si layer on 2μm of thermal oxide. The parts were first defined by reactive ion etching through the bonded layer. The movable parts were perforated to allow release. The meltable pads were formed by patterning a 12μm thick layer of Hoechst AZ4562 photoresist. The mechanical parts were undercut using buffered HF, and wash water was removed by freeze drying. Self-assembly was carried out by heating at 150°C for five minutes.

After assembly, the structure was sputtered coated with 500Å Al metal. This step increased the reflectivity of the mirror, and provided a direct electrical connection between parts 1 and 2, which are otherwise linked only by insulating pads of photoresist. However, the large lateral etch obtained during removal of the buried oxide ensured that a continuous conducting film was not obtained between parts 1 and 4, so that they remained electrically isolated. Electrical connection to the two halves of the drive could then be made by contacting to parts 1 and 4.

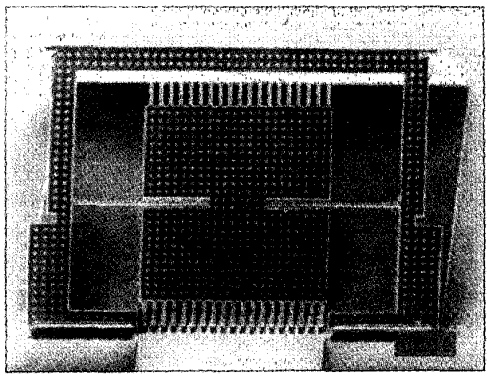

Fig. 2 *Device fabricated in bonded silicon-on-insulator, after self-assembly*

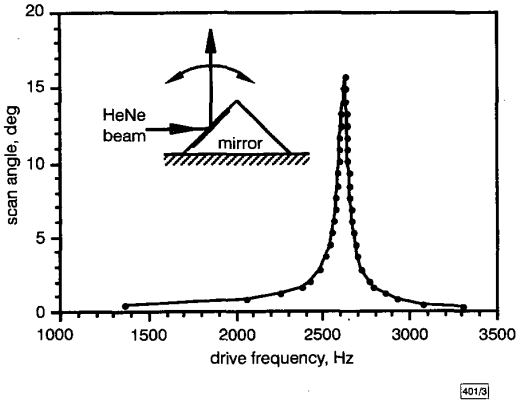

Fig. 3 *Variation of scan angle with frequency, obtained using 175 V p-p sinusoidal drive*

Fig. 2 shows the completed structure, highlighting its three-dimensional nature. Melted resist pads may be seen on either side of the mirror frame (part 2), the base width of which is 1mm. The mirror itself measures 456μm parallel to and 496μm perpendicular to the axis of rotation. The moving half of the comb contains 19 fingers, each 8μm wide and 60μm long, and the electrode gap is